Metallomics

PAPER

View Article Online
View Journal | View Issue

Cite this: *Metallomics*, 2014, 6, 1460

Antitumor properties and mechanisms of mitochondria-targeted Ag(I) and Au(I) complexes containing N-heterocyclic carbenes derived from cyclophanes†

Yi Li, Gao-Feng Liu,* Cai-Ping Tan, Liang-Nian Ji and Zong-Wan Mao*

Received 19th February 2014,
Accepted 17th April 2014

DOI: 10.1039/c4mt00046c

www.rsc.org/metallomics

Metal/N-heterocyclic carbene (NHC) complexes hold great opportunities for the development of novel antitumor metallodrugs. Herein, four Ag(I) and Au(I) complexes containing NHCs derived from cyclophanes have been prepared and characterized as potential anticancer agents. These complexes show higher cytotoxicity than cisplatin against several cancer cell lines including a cisplatin-resistant cell line. The Au(I) complexes display higher anticancer activity than the corresponding Ag(I) complexes. Moreover, all the complexes are less cytotoxic than cisplatin on the normal human liver cell line LO2. Intracellular distribution studies show that these complexes are selectively localized in the mitochondria, especially for the Au(I) complexes. Interestingly, although both Ag(I) and Au(I) complexes can influence mitochondrial integrity, they induce cancer cell death through different mechanisms. The Ag(I) complexes mainly induce caspase- and reactive oxygen species (ROS)-independent early apoptosis. However, Au(I) complexes induce both early apoptosis and late apoptosis through caspase- and ROS-dependent pathways. These studies may open up an avenue for a better understanding of the impact of metal centers on antitumor potentialities and mechanisms.

Introduction

Platinum-based drugs, such as cisplatin and carboplatin, are widely used drugs in cancer chemotherapy. However, the clinical applications of platinum anticancer agents are hindered by several drawbacks, *e.g.*, severe side effects, intrinsic and acquired drug resistance.[1] The development of non-platinum based metal anti-cancer drugs offers the prospect of exploiting novel metallo-chemotherapeutics that can overcome the limitations of platinum-based drugs.[2,3]

Metal–NHC complexes have played a significant role in catalytic processes.[4–7] NHC can form strong coordinate covalent bonds with various transition metal centres through σ-donation and π-back-donation.[8–10] The extra stability makes metal–NHC complexes promising candidates for drug development. In the past decade, increasing interest has been drawn towards the antitumor activities of metal–NHC complexes.[11–13]

Silver compounds have long been used as antimicrobial agents.[14,15] Due to the high stability of Ag–NHCs, they can overcome the problems associated with conventional silver antibiotics such as resistance and fast loss of activity.[16–21] Some of them exhibit antitumor activity both *in vitro* and *in vivo*.[22–27] However, there are relatively few reports on the research of the mechanism, and the mode of action of Ag–NHC complexes remains unclear.[28]

Au(I)– and Au(III)–NHCs exhibit a varied range of biological activities, including antiarthritic,[29,30] antimicrobial[31] and antitumor[32–40] activities. It has been proved that Au(I)–NHC complexes can induce cell death by targeting the mitochondrial-related pathways.[41–43] Preliminary studies on the mode of action show that gold NHC complexes can act through the inhibition of enzymes including thioredoxin reductase (TrxR), Estrogen Receptor (ER) and cyclooxygenase (COX).[28]

Herein, four Ag(I)– and Au(I)–NHC complexes containing N-heterocyclic carbene ligands derived from imidazolium-linked cyclophanes have been designed and synthesized (Fig. 1). These imidazolium-linked bis(carbene) ligands in which the NHC units are part of a rigid cyclophane skeleton exhibit excellent stability,[44] and the fluorescence of anthracene group is likely to enhance the fluorescence properties of the complexes. The primary aim of this study is to illustrate the effect of different ligands and metal centres on the antitumor activities and mechanisms of

MOE Key Laboratory of Bioinorganic and Synthetic Chemistry, School of Chemistry and Chemical Engineering, Sun Yat-sen University, Guangzhou, 510275, P. R. China. E-mail: cesmzw@mail.sysu.edu.cn, liugaof@mail.sysu.edu.cn; Fax: +86-20-8411-2245

† Electronic supplementary information (ESI) available: The crystallographic details and additional material for the biological studies. CCDC 980882–980885. For ESI and crystallographic data in CIF or other electronic format see DOI: 10.1039/c4mt00046c

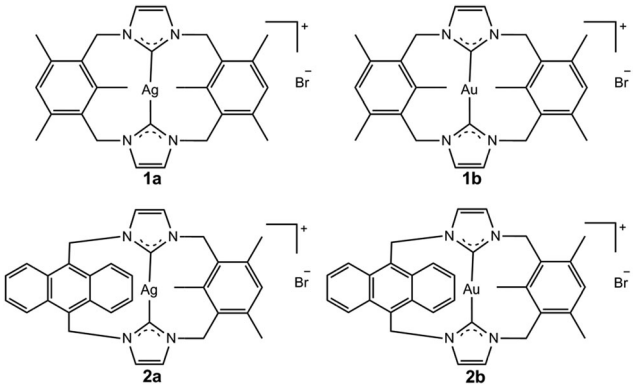

Fig. 1 Chemical structures of metal–NHC complexes studied in this work.

metal–NHC complexes. The cytotoxicity of these metal–NHCs is assessed on several cancer cell lines including a cisplatin-resistant cell line. In order to further illustrate the possible anticancer mechanisms of these complexes, their impacts on cell cycle distribution, mitochondrial integrity, ROS level and expressions of several key regulators of apoptosis are evaluated. The results obtained give a new insight into the differences in anticancer mechanisms between Ag(I)– and Au(I)–NHC complexes.

Results and discussion

Synthesis and characterization

The silver complexes were prepared by the direct reaction of N-heterocyclic carbene precursors with Ag_2O in a solvent mixture of dichloromethane–methanol in the dark (Scheme S1, ESI†). The gold complexes were obtained *via* the carbene-transfer reaction of the corresponding silver complexes with $(SMe_2)AuCl$ in dichloromethane.[45] The complexes and ligands were characterized using ESI-MS, ^{1}H-NMR, ^{13}C-NMR and elemental analysis.

The formations of the NHC complexes are confirmed by the disappearance of a H2 proton and an upfield chemical shift of H4/H5 protons in their ^{1}H NMR spectra.[10] The X-ray crystallography structures of **1a**, **1b**, $\mathbf{L^1}$ and $\mathbf{L^2}$ were obtained as hexafluorophosphate salts by means of anion exchange reaction with ammonium hexafluorophosphate in methanol and slow evaporation of concentrated acetonitrile solution (Fig. 2 and Table S1, ESI†). The geometries of the silver atoms in **1a**′ and gold atoms in **1b**′ are nearly linear. The bond angle of C1–Ag1–C2 is 178.04(18)° and the bond angle of C13–Au1–C15 is 179.4(3)°. The bond distances of Ag1–C1 and Ag1–C2 are 2.113(4) Å and 2.111(4) Å, respectively. The bond distances of Au1–C13 and Au1–C15 are 2.063(8) Å and 2.072(8) Å, respectively. As shown in Fig. 2 and Table S2 (ESI†), the structure of the Ag complex **1a**′ is similar to that of the Au complex **1b**′. The electronic absorption and emission properties of **2a** and **2b** in methanol solutions at 298 K are shown in Fig. S1 (ESI†).

It has been proved that hydrolysis is the key activation step for cisplatin and its derivatives inside the cell. However, for many metal complexes, hydrolysis is supposed to be an unfavourable process with regard to their anticancer efficiencies. It has been reported that Ag–NHC complexes can undergo hydrolysis in aqueous solutions.[46,47] The time-dependent absorption spectra of **1–2** in 100 mM NaCl solutions (a similar concentration to that in blood plasma) at 298 K are shown in Fig. S2 (ESI†). Obvious time-dependent changes in the absorption spectra of Ag–NHC complexes **1a** and **2a** can be observed, which suggests hydrolysis of the complexes. Time-dependent absorption spectra of **2a** show a decrease in the intensity of the peaks at 402 nm, 380 nm, 362 nm, along with an increase in the intensity of the peaks at 396 nm, 375 nm, 356 nm, 339 nm. Meanwhile, a decrease in the absorption intensity at *ca.* 270 nm in the time-dependent spectra of **1a** can also be observed. The hydrolysis rates of the complexes follow the order: **2a** > **1a**. However, no obvious changes in the absorption spectra of Au–NHC complexes **1b** and **2b** can be observed for 12 h. Ag–NHC complexes **1a** ($t_{1/2}$ = 1.8 ± 0.1 h) and **2a** ($t_{1/2}$ = 3.8 ± 0.2 h) show much faster rates of hydrolysis than the Au–NHC complexes **1b** and **2b**, which may partially explain the differences in antitumor properties between Ag–NHC and Au–NHC complexes.

The stability of complexes **1a–b** and **2a–b** in aqueous solutions were also analysed using ESI-MS (Fig. S3, ESI†). Complexes were dissolved in DMSO and then diluted with water. The solutions were subjected to ESI-MS analysis immediately (Fig. S3A, ESI†). After 2 days, these solutions were subjected to ESI-MS analysis again (Fig. S3B, ESI†). The results show that Ag–NHC complexes **1a** and **2a** were relatively unstable in water and ESI-MS analysis of the product indicate the cleavage of the Ag–C bonds and the generation of carbene ligands. However, the Au–NHC

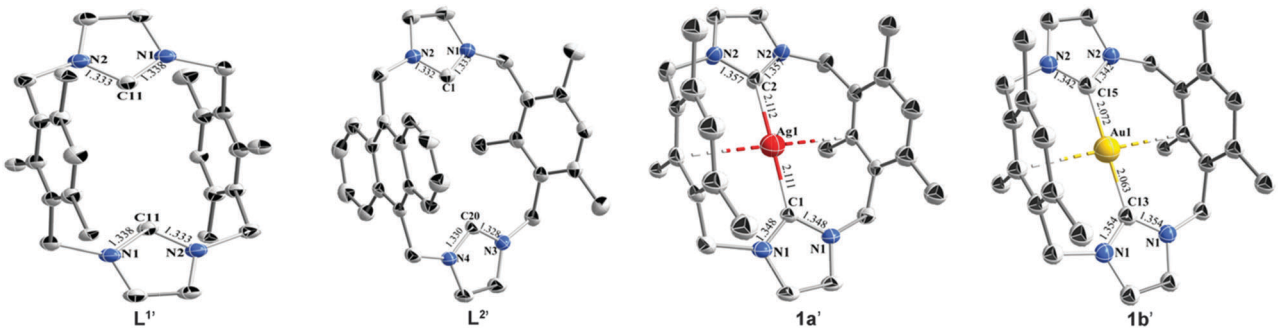

Fig. 2 X-ray crystal structures of $\mathbf{L^{1\prime}}$, $\mathbf{L^{2\prime}}$, **1a**′ and **1b**′. The hydrogen atoms and counter ions are omitted for clarity.

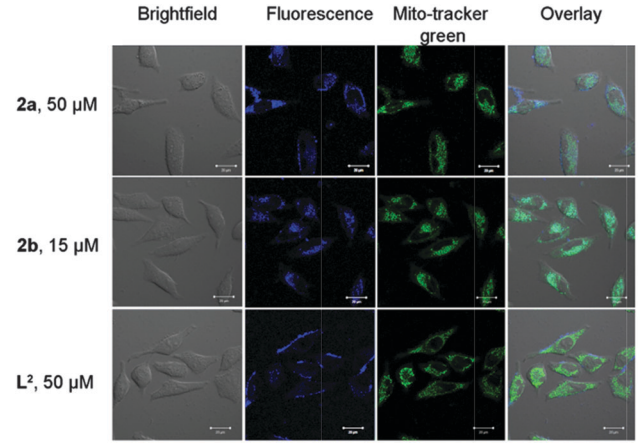

Fig. 3 Determination of intercellular localization of compound by confocal microscopy (63× oil-immersion objective lens). **2a**, **2b** and $\mathbf{L^2}$ were excited at 405 nm (blue). Mito-tracker green was excited at 488 nm (green).

complexes **1b** and **2b** were very stable and did not hydrolyze under the same conditions, as compared with the corresponding Ag–NHC complexes **1a** and **2a**.

Intracellular localization

The intercellular distribution of drugs can influence their cytotoxicity and mechanism. It has been reported that metal–NHC complexes accumulate mainly in the cytoplasm, and some of them can selectively localize on organelles, including mitochondria,[40,48–51] lysosomes[52] and the endoplasmic reticulum.[53] Owing to the fluorescence of anthracene, HeLa cells were incubated with ligand $\mathbf{L^2}$ and complexes **2a**, **2b** at the indicated concentrations for 1 h at 37 °C, and fluorescence was analysed using a confocal microscope (Fig. 3). Significant blue fluorescence of complexes **2a** and **2b** was mainly detected in the cytoplasm. Under the same experimental conditions, no fluorescent signals were observed for ligand $\mathbf{L^2}$ in the cytoplasm. The specific cellular locations of the fluorescence were further studied by co-localization analysis with organelle-specific stains, including mito-tracker green and lyso-tracker green. It was found that the Au complex **2b**-treated cells was localized in the mitochondria and could be specifically stained with mito-tracker green (Pearson's correlation coefficient R = 0.82), but not in the lysosomes (Fig. S4, ESI†). These result indicated that these Ag(I) and Au(I) NHC complexes induced cell death probably through the mitochondrial pathway and DNA may not be the target. Different from platinum-anticancer drugs, these complexes may exert their anticancer activity through interaction with proteins in the cytoplasm.[39,50,54]

Antiproliferative activity

The *in vitro* cytotoxicity of the complexes was determined using 3-(4,5-dimethylthiazol-2-yl)-2,5-diphenyltetrazolium bromide (MTT) assays. The compounds were tested for their antiproliferative activity against human cervical carcinoma (HeLa), human lung adenocarcinoma epithelial (A549), cisplatin-resistant A549 (A549R), human breast carcinoma (MDA-MB-231) and human normal liver (LO2) cell lines 48 h post-treatment. For comparison purpose, ligands $\mathbf{L^1}$, $\mathbf{L^2}$ and cisplatin were evaluated under the same experimental conditions.

Table 1 IC_{50} values of tested compounds towards different cell lines[a]

	IC_{50} (μM)				
Compound	HeLa	A549	MDA-MB-231	A549R	LO2
$\mathbf{L^1}$	>100	>100	>100	>100	>100
$\mathbf{L^2}$	>100	>100	>100	>100	>100
1a	19.1 ± 1.9	19.2 ± 4.0	22.0 ± 0.5	20.1 ± 1.2	91.3 ± 4.2
1b	3.3 ± 0.4	10.2 ± 2.5	4.5 ± 0.3	16.0 ± 2.5	65.1 ± 3.1
2a	12.4 ± 1.9	16.5 ± 0.6	14.3 ± 0.2	16.7 ± 0.8	64.6 ± 3.3
2b	4.5 ± 0.3	15.2 ± 1.5	4.4 ± 0.4	13.2 ± 0.8	35.6 ± 1.0
Cisplatin	18.8 ± 3.0	26.7 ± 1.5	17.2 ± 3.0	67.0 ± 5.4	11.6 ± 0.7

[a] IC_{50} values are drug concentrations necessary for 50% inhibition of cell viability. Data are presented as means ± standard deviations (SD) obtained in at least three independent experiments and drug treatment period was 48 h.

As shown in Table 1, all of the Ag(I) and Au(I) complexes displayed superior or comparable anticancer activity against cancer cell lines and lower cytotoxicity towards normal liver LO2 cells as compared with cisplatin. Notably, Au(I) complexes **1b** and **2b** showed superior antiproliferative activity over the corresponding Ag(I) complexes **1a** and **2a**. One of the possible reasons is that Au–NHC complexes are more stable in aqueous solutions compared with Ag–NHC complexes. Among the cancer cells tested, Au(I) complexes **1b** and **2b** also display selectivity for HeLa (IC_{50} = 3.3 ± 0.4 μM and 4.5 ± 0.3 μM for **1b** and **2b**, respectively) and MDA-MB-231 (IC_{50} = 4.5 ± 0.3 μM and 4.4 ± 0.4 μM for **1b** and **2b**, respectively) cell lines. Their ability to differentiate among these cell types could be useful in therapeutic applications.

These Ag(I)– and Au(I)–NHC complexes were significantly more active than cisplatin in both cisplatin-sensitive A549 cells and cisplatin-resistant A549R cells, indicating that these complexes could overcome cisplatin resistance.

The ligand $\mathbf{L^1}$ and $\mathbf{L^2}$ exhibited IC_{50} values higher than 100 μM, the highest concentration tested for these compounds, which confirmed that the formation of metal complexes was necessary for the antiproliferative activity. Hence, the synergistic effect of the metal centres and the NHC ligands clearly has a role in the cytotoxicity of metal–NHC complexes.[27]

Cell-cycle arrest

The cytotoxicity of metal-based drugs is often associated with cell cycle perturbation, which finally leads to cell death execution. It has been recently reported that metal–NHC complexes can induce cell cycle arrest.[34,55,56] To further elucidate the antiproliferative mechanisms of these complexes, HeLa cells were treated with complexes **1–2** at the indicated concentrations for 24 h and cell cycle analysis was performed by propidium iodide (PI) staining and flow cytometry (Fig. S5, ESI†). Cell distribution analysis revealed that complexes **1–2** had no obvious effects on the cell cycle. Significant increases in the percentage of cells in the sub-G1 phase, indicative of apoptosis, were caused by treatment of the complexes at elevated concentrations. The proportion of cells in the sub-G1 phase caused by Ag–NHCs complexes was higher than that caused by Au–NHCs under the same conditions.

Therefore, no distinct modification in the cell-cycle distribution revealed that complexes **1–2** are not genotoxic.[49]

Induction of apoptosis

Apoptosis is often characterized by some biochemical and morphological features, such as plasma membrane blebbing, loss of mitochondria transmembrane potential, cytoplasmic shrinkage and nuclear fragmentation.[57] It has been demonstrated that lipophilic and cationic Au(I)–NHCs can selectively induce apoptosis through interaction with mitochondrial selenoproteins,[34,36,39,50,58,59] and Ag(I)–NHCs can induce depolarization of mitochondrial inner membrane potential to elicit early apoptosis.[49] Annexin V was used to detect phosphatidylserine externalization, a hallmark of the early apoptosis.[60] HeLa cells were treated with complexes **1a–b** and **2a–b** at different concentrations for 24 h and double-labelled with annexin V and PI. Early apoptotic cells are annexin V-positive but PI-negative, because the plasmic membrane is intact while phosphatidylserine is externalized. Late apoptotic and necrotic cells can be stained by both PI and annexin V. Flow cytometric analysis indicated that all of the complexes could induce apoptosis (Fig. 4). The results indicated that Ag(I)–NHCs **1a** and **2a** mainly induced early apoptosis at higher concentration, especially for complex **2a** (71.4% ± 2.3 cells in early apoptosis). However, the Au(I)–NHCs **1b** and **2b** were more inclined to induce early apoptosis and late apoptosis even at lower concentrations as compared with Ag(I)–NHCs. These results demonstrate that Ag(I) and Au(I)–NHCs can induce cell death *via* the apoptotic way, but the pathways in the apoptosis induced by them might be different.

Impact on mitochondrial integrity

Maintenance of the integrity of the mitochondrial membrane plays a vital role in cell survival. During the apoptosis process, several key events usually occur in mitochondria, including the release of caspase activators and the loss of mitochondrial membrane potential (MMP). It has been reported that cationic complexes have the ability to readily pass through the lipid membrane of mitochondria and accumulate in mitochondria, leading to mitochondria-mediated apoptosis.[32,42,43,50,59,61] In order to investigate whether mitochondrial dysfunction was involved in apoptosis induced by these NHC complexes, the changes in MMP were detected by flow cytometry in cells stained with 5,5′,6,6′-tetrachloro-1,1′-3,3′-tetraethyl-benzimidazolylcarbocyanine iodide (JC-1), a cationic dye which selectively stains polarized mitochondria. Mitochondrial depolarization is indicated by a decrease in the red/green fluorescence intensity ratio (I_{585nm}/I_{530nm}).[62] As shown in Fig. 5A, treatment of complexes **1–2** for 4 h significantly decreased the intensity ratios of red/green fluorescence as compared with the vehicle-treated (1% DMSO) cells. These results proved that Ag(I)– and Au(I)–NHCs likely induce apoptosis through modification of MMP, and subsequent release of mitochondrial material, such as cytochrome *c* and apoptosis-induced factor. The less cytotoxic silver complexes could decrease the red/green fluorescence intensity ratio more profoundly than the corresponding gold complexes at the indicated concentrations. This phenomenon further suggested that the mechanism of action might be different.

Elevation of intracellular ROS levels

Mitochondrial dysfunction and ROS accumulation are two closely related events in the intrinsic apoptosis pathway.[63] It has been reported that gold–NHCs can markedly increase the intracellular ROS levels.[36] The effects of complexes **1a–b** and **2a–b** on intracellular ROS levels were examined by 2′,7′-dichlorofluorescein (DCF) fluorescence assay measured by flow cytometry (Fig. 5B). After a 4 h treatment, HeLa cells were stained with 2′,7′-dichlorofluorescein diacetate (H_2DCFDA), a nonfluorescent compound which can be converted into the highly fluorescent DCF species in the presence of intracellular ROS. The results show that Ag(I)–NHCs have no obvious effects on intracellular ROS levels, but gold–NHCs cause an approximately 4- to 6-fold increase in DCF fluorescence signals as compared with the vehicle-treated cells. In order to examine whether ROS played a role in

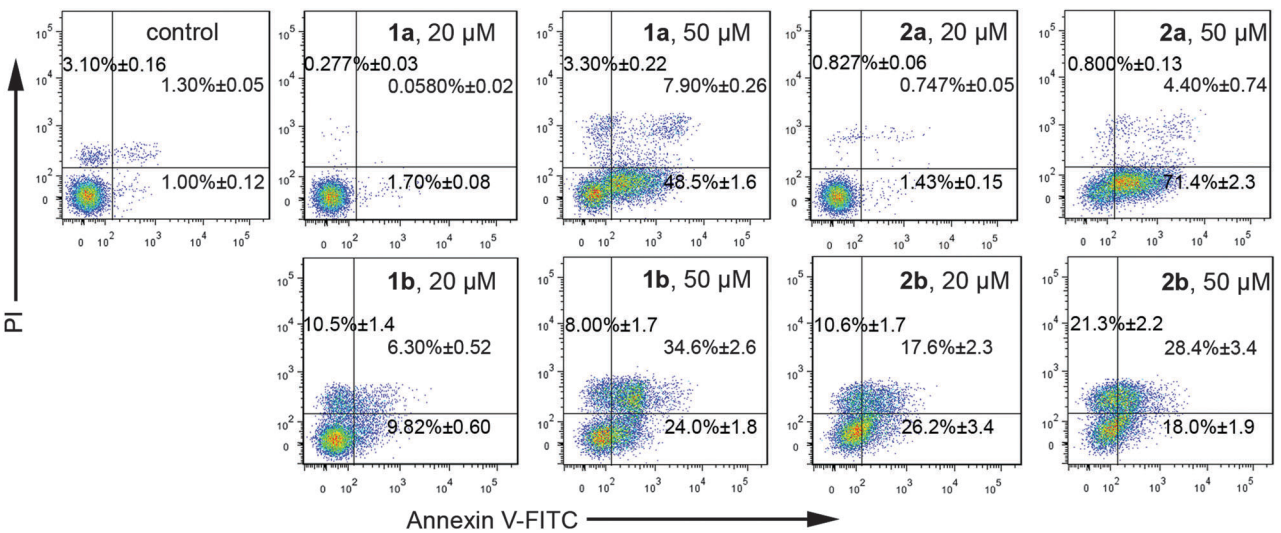

Fig. 4 Flow cytometric quantification of annexin V and PI double labeled HeLa cells after treatment with **1a–b** and **2a–b** (50 μM) for 24 h.

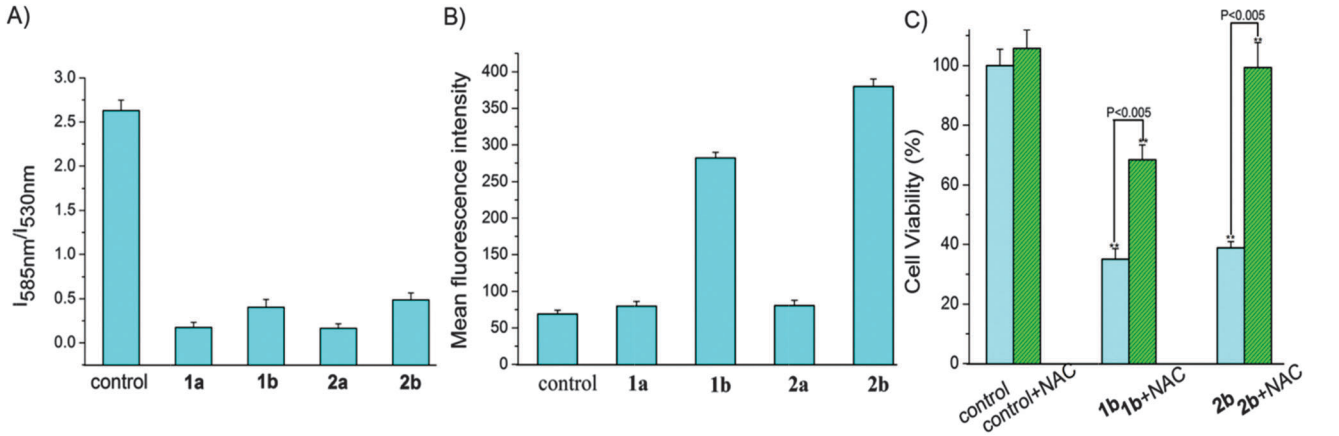

Fig. 5 (A) Impact of complexes **1–2** on MMP. The fluorescent intensity ration of HeLa cells treated with **1a–b** and **2a–b** at concentrations of 50 μM for 4 h. (B) Intracellular ROS production in HeLa cells after a 4 h treatment with complexes **1–2** at a concentration of 50 μM. (C) Effects of NAC (10 mM) on **1b**- and **2b**-induced cytotoxicity. HeLa cells were exposed to **1b** (3.125 μM) and **2b** (6.25 μM) with or without antioxidants for 48 h. Cell viability was assessed using a MTT assay.

Au(I)-elicited cell death, we used *N*-acetylcysteine (NAC, 10 mM), a ROS scavenger, to examine their effect on cell viability after treatment of Au–NHC complexes. The results showed that NAC substantially suppressed ROS accumulation and reduced the cytotoxicity of **1b** and **2b** in HeLa cells (Fig. 5C), suggesting that cell death induced by gold complexes **1b** and **2b** is ROS-dependent.

Caspase-3/7 activation

During the apoptosis process, the activation of caspase-3/7 is generally regarded as one of the most obviously characteristics in many cell types.[64] To get insight into the mechanism of complexes **1–2** induced apoptosis, a caspase-3/7 activity assay was carried out. As shown in Fig. 6A and B, 50 μM cisplatin and Au(I)–NHC complexes **1b**, **2b** markedly stimulated the activation of caspase-3/7 after a 12 h treatment. In contrast, Ag(I)–NHC complexes **1a** and **2a** had only marginal effect on the activation of caspase-3/7. The results suggested that the activation of apoptosis by these Au(I)–NHC complexes was caspase-dependent.[40] However, apoptosis induced by Ag(I)–NHC complexes was caspase-independent.[49]

Furthermore, the western blot experiment also demonstrated that Au–NHC complexes **1b** and **2b** caused a dose-dependent

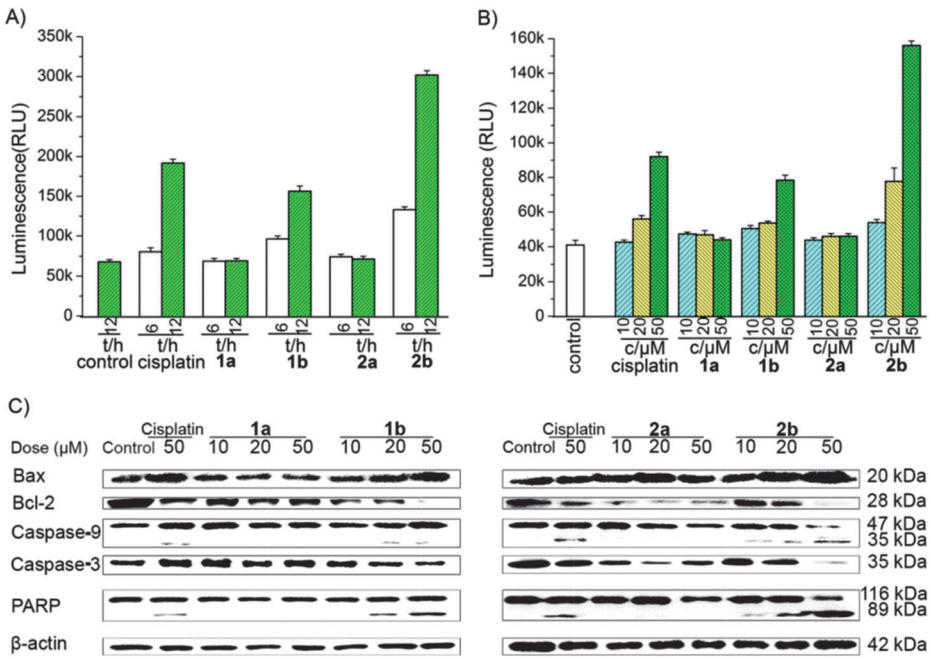

Fig. 6 (A) Activation of caspases-3/7. HeLa cells were exposed to cisplatin and complexes **1–2** at 50 μM for 6 h, 12 h and 24 h. (B) Caspases-3/7 activation experiments. HeLa cells were exposed to cisplatin and complexes **1–2** at the concentrations of 10 μM, 20 μM and 50 μM for 12 h, respectively. (C) Western blot results after treating HeLa cells with cisplatin and complexes **1–2** for 12 h.

increase in the protein levels of bax, cleaved caspase-9, cleaved poly(ADP-ribose)polymerase (PARP). Decreased expression levels of caspase-3 were also observed (Fig. 6C). A dose-dependent increase in bax expression accompanied by decrease in Bcl-2 expression were observed after treatment of cells with Ag(I)–NHC complexes. However, activation of caspases was not observed for Ag(I)–NHC complexes **1a** and **2a**. Taken together, these results suggested that complexes **1–2** induce apoptosis probably through the mitochondrial mediated pathway. Au(I)–NHC complexes **1b** and **2b** triggered apoptosis through a caspase-dependent mechanism, while Ag–NHC complexes **1a** and **2a** through a caspase-independent mechanism.

Conclusions

In conclusion, we have synthesized and characterized four cationic Ag(I)– and Au(I)–NHC complexes derived from cyclophanes. These Ag(I)– and Au(I)–NHC complexes have similar structures; however, they exert their anticancer activity through different mechanisms. The Au(I)–NHC complexes are more stable in aqueous solutions and can selectively localize in mitochondria.

All of these complexes exhibit potent antitumor activity toward human cancer cell lines, including cisplatin resistant lines. The Au–NHC complexes display higher antiproliferative activity and selectivity as compared with corresponding Ag–NHC complexes and cisplatin. Further mechanism studies show that these complexes have no effect on the cell cycle and can induce apoptosis in cancer cells. Ag(I) complexes mainly induce early apoptosis, but Au(I) complexes induce cancer cell death through early and late apoptosis. These Ag(I)– and Au(I)–NHC complexes can markedly reduce the MMP, indicating that they can induce apoptosis through the mitochondrial pathway. Au(I)–NHC complexes can increase the intracellular ROS levels and their cytotoxicity is ROS-dependent. In addition, Au–NHC complexes can stimulate the activation of caspase-3/7 and trigger apoptosis through a caspase-dependent mechanism. In contrast, Ag–NHCs complexes trigger apoptosis *via* a caspase- and ROS-independent pathway. These studies may give some hints on the different anticancer mechanisms in metal–NHC complexes bearing different metal centres.

Experimental section

General procedures

All starting materials were used as received from commercial sources unless otherwise indicated. Solvents were purified and degassed by standard procedures. The ligand $\mathbf{L^1}$,[65] 9,10-bis(bromomethyl)anthracene,[66] and $(SMe_2)AuCl$[67] were synthesized according to procedures in the literature. The purity of synthesized compounds was confirmed by elemental analysis, and all of them showed purity greater than 95%.

NMR spectra were recorded on a Mercury Plus 300 spectrometer. Shifts are referenced relative to the internal solvent signals. Microanalysis (C, H, and N) was carried out using an Elemental Vario EL CHNS analyzer (Germany). Fluorescence spectra were recorded on a Shimadzu RF5301 spectrofluorophotometer. UV-vis spectra were recorded on a Varian Cary 300 spectrophotometer. ESI-MS spectra were recorded on a Thermo Finnigan LCQ DECA XP spectrometer (USA). The quoted *m*/*z* values represent the major peaks in the isotopic distribution. Fluorescence microscopy was performed on a LSM 710 (Carl Zeiss). For MTT assays, the absorbance was quantified using an Infinite M200 microplate reader (Switzerland).

X-ray crystallographic analysis. To a solution of **1a**, **1b** and $\mathbf{L^1}$, $\mathbf{L^2}$ in methanol was added 2 molar equiv. of NH_4PF_6, respectively. The obtained precipitate dissolved in acetonitrile and slowly evaporated solutions to give crystals of **1a**, **1b**, $\mathbf{L^1}$ and $\mathbf{L^2}$ suitable for X-ray analysis. The data were collected at 293 K on a Rigaku Pilatus diffractometer equipped with Mo Kα radiation (λ = 0.71073 Å). Structure solution and refinement were performed using the SHELX-97 suite program. In the final stage of least-squares refinement, non-hydrogen atoms were refined anisotropically. Crystallographic data and details of the data collection and structure refinements are listed in Table S1 (ESI†). Selected bond distances and angles of the compounds are listed in Table S2 (ESI†).

Synthesis of ligands and complexes

1a. To a solution of the ligand $\mathbf{L^1}$ (117 mg, 0.2 mmol) in a mixture of CH_2Cl_2 (21 mL) and methanol (6 mL) was added Ag_2O (70 mg, 0.3 mmol). The reaction mixture was stirred at room temperature for 24 h under the exclusion of light to give a light brown precipitate. The suspension was filtered over Celite, and the clear solvent was concentrated to 2 mL approximately under reduced pressure, then about 20 mL ether was added to give an off-white precipitate. The precipitate was filtered, washed with diethyl ether, and then dried under vacuum (90 mg, yield 73.5%). ^{1}H NMR (300 MHz, d_6-DMSO, TMS) δ 7.61 (s, 4H), 6.83 (s, 2H), 5.26 (s, 8H), 1.87 (s, 18H); ^{13}C NMR (75 MHz, d_6-DMSO, TMS) δ 179.36, 138.13, 137.44, 131.63, 131.43, 123.24, 48.99, 19.48, 18.11; ESI-MS: calcd. for *m*/*z* 531.2(^{107}Ag) and 533.2(^{109}Ag) $[M - Br]^+$. Found: *m*/*z* 531.4(^{107}Ag) and 533.3(^{109}Ag) $[M - Br]^+$; elemental analyses calcd (%) for $C_{28}H_{32}AgBrN_4 \cdot 0.5H_2O$: C, 54.12; H, 5.35; N, 9.02; found: C, 54.16; H, 5.52; N, 8.72.

1b. A mixture of **1a** (0.305 mg, 0.5 mmol) and $(SMe_2)AuCl$ (116 mg, 0.5 mmol) was taken in dichloromethane (21 mL) and methanol (6 mL), stirred at room temperature for 12 h under the exclusion of light. The suspension was filtered over Celite, and the clear solvent was concentrated to 2 mL approximately under reduced pressure, then about 20 mL ether was added to give an off-white precipitate. The precipitate was filtered, washed with diethyl ether, and then dried under vacuum (219 mg, yield 62.4%). ^{1}H NMR (300 MHz, d_6-DMSO, TMS) δ 7.61 (s, 4H), 6.79 (s, 2H), 5.28 (s, 8H), 1.84 (s, 18H); ^{13}C NMR (75 MHz, d_6-DMSO, TMS) δ 179.12, 139.44, 137.66, 131.00, 130.75, 123.35, 48.93, 18.92; ESI-MS: calcd for *m*/*z* 621.2 $[M - Br]^+$. Found: *m*/*z* 621.3 $[M - Br]^+$; elemental analyses calcd. (%) $C_{28}H_{32}AuBrN_4 \cdot 2H_2O \cdot CH_2Cl_2$: C, 42.35; H, 4.66; N, 6.81; found: C, 42.49; H, 4.66; N, 6.93.

L^2. A solution of 2,4-bis(imidazol-1-ylmethyl)mesitylene (105 mg, 0.410 mmol) in acetone (20 mL) was added dropwise to a solution of 9,10-bis(bromomethyl)anthracene (149 mg, 0.376 mmol) in acetone (40 mL) at room temperature and the mixture was stirred for 3 days. The precipitate was filtered, washed with acetone, and then dried under vacuum (218 mg, yield 90.1%). ^{1}H NMR (300 MHz, d_6-DMSO, TMS) δ 8.34 (dd, J = 6.8, 3.2 Hz, 4H), 8.31 (t, J = 1.7 Hz, 2H), 7.91 (t, J = 1.7 Hz, 2H), 7.61 (dd, J = 6.9, 3.1 Hz, 4H), 6.86 (s, 1H), 6.61 (s, 4H), 6.38 (s, 2H), 5.16 (s, 4H), 2.07 (s, 6H), 1.15 (s, 3H); ^{13}C NMR (75 MHz, d_6-DMSO, TMS) δ 140.48, 138.52, 133.46, 130.39, 128.43, 128.15, 128.01, 125.03, 124.67, 123.72, 48.21, 46.71, 20.13, 14.56; ESI-MS: calcd for m/z 563.2(^{79}Br) and 565.2(^{81}Br) $[M - Br]^+$ and 242.1 $[M - 2Br]^{2+}$. Found: m/z 562.9(^{79}Br) and 564.9(^{81}Br) $[M - Br]^+$ and 242.2 $[M - 2Br]^{2+}$; elemental analyses calcd. (%) for $C_{33}H_{32}Br_2N_4 \cdot 2.5H_2O$: C, 57.49; H, 5.41; N, 8.13; found C, 57.63; H, 5.63; N, 7.89%.

2a. To a solution of the ligand L^2 (128 mg, 0.2 mmol) in a mixture of CH_2Cl_2 (21 mL) and methanol (12 mL) was added Ag_2O (70 mg, 0.3 mmol). The reaction mixture was stirred at room temperature for 24 h under the exclusion of light to give a light brown precipitate. The suspension was filtered over Celite, and the clear solvent was concentrated to 2 mL approximately under reduced pressure, then about 20 mL ether was added to give a yellow precipitate. The precipitate was filtered, washed with diethyl ether, and then dried under vacuum (97 mg, yield 72.4%). ^{1}H NMR (300 MHz, d_6-DMSO, TMS) δ 8.33 (d, J = 28.3 Hz, 4H), 7.71 (s, 2H), 7.57 (s, 2H), 7.49 (s, 4H), 6.65 (s, 1H), 6.42 (s, 4H), 5.01 (d, J = 17.2 Hz, 4H), 1.87 (s, 3H), 1.80 (s, 6H). ^{13}C NMR (75 MHz, d_6-DMSO, TMS) δ 176.50, 137.73, 136.40, 131.78, 131.31, 130.39, 127.36, 126.68, 125.01, 123.98, 48.80, 47.02, 19.80, 17.22; ESI-MS: calcd. for m/z 589.2(^{107}Ag) and 591.2(^{109}Ag) $[M - Br]^+$. Found: m/z 589.4(^{107}Ag) and 591.3(^{109}Ag) $[M - Br]^+$. Elemental analyses calcd. (%) for $C_{33}H_{30}AgBrN_4 \cdot 2H_2O$: C, 56.11; H, 4.85; N, 7.93; found C, 56.35; H, 5.03; N, 7.66%.

2b. A mixture of **2a** (351 mg, 0.5 mmol) and $(SMe_2)AuCl$ (116 mg, 0.5 mmol) was taken in dichloromethane (21 mL) and methanol (12 mL), stirred at room temperature for 12 h under the exclusion of light. The suspension was filtered over Celite, and the clear solvent was concentrated to 2 mL approximately under reduced pressure, then about 20 mL ether was added to give a yellow precipitate. The precipitate was filtered, washed with diethyl ether, and then dried under vacuum (258 mg, yield 67.9%). ^{1}H NMR (300 MHz, d_6-DMSO, TMS) δ 8.31 (d, J = 14.6 Hz, 4H), 7.70 (s, 2H), 7.68 (s, 2H), 7.47 (dd, J = 6.2, 3.1 Hz, 4H), 6.65 (s, 1H), 6.50 (d, J = 7.7 Hz, 4H), 5.08 (d, J = 12.1 Hz, 4H), 2.04 (s, 3H), 1.81 (s, 6H); ^{13}C NMR (75 MHz, d_6-DMSO, TMS) δ 179.53, 134.92, 134.74, 132.90, 132.30, 129.13, 128.93, 127.54, 126.69, 126.18, 51.27, 50.52, 21.34, 20.74; ESI-MS: calcd. for m/z 679.2 $[M - Br]^+$. Found: m/z 679.3 $[M - Br]^+$; elemental analyses calcd (%) $C_{33}H_{30}AuBrN_4 \cdot 2H_2O$: C, 49.82, H, 4.31; N, 7.04; found C, 49.94; H, 4.42; N, 7.27%.

Cell lines and growth inhibitory assay

HeLa, A549, A549R, MDA-MB-231 and LO2 cells were obtained from Experimental Animal Centre of Sun Yat-sen University (Guangzhou, China). Cells were maintained in DMEM (Dulbecco's modified Eagle's medium, Gibco BRL) for HeLa, MDA-MB-231, LO2; and RPMI 1640 (Roswell Park Memorial Institute medium 1640, Gibco BRL) medium for A549 and A549R, which contained 10% FBS (fetal bovine serum, Gibco BRL), 100 μg mL^{-1} streptomycin, and 100 U mL^{-1} penicillin (Gibco BRL). The cells were cultured in a humidified incubator, which provided an atmosphere of 5% CO_2 and 95% air at a constant temperature of 37 °C. A549R cells were cultured in medium containing cisplatin to maintain the resistance.

The cell growth inhibitory effects of the Ag(I)– and gold(I)–NHC complexes and cisplatin were determined by a MTT cytotoxicity assay. Briefly, the compounds were freshly dissolved in DMSO (1%, v/v), and diluted with fresh media immediately. Cells were cultured in 96-well plates (Corning, USA). The cells were incubated with series concentrations of the compounds for 44 h. Then, 20 μL of MTT solution (5 mg mL^{-1}) was then added to each well, and the plates were incubated for an additional 4 h. The media was carefully removed and 150 μL DMSO was added per well and shaken for 10 min. The absorbance at 490 nm was measured using a microplate reader (Infinite M200, Tecan, Männedorf, Switzerland). Growth inhibition was evaluated by IC_{50} (concentration of a drug causing 50% inhibition of cell growth). Each growth inhibition experiment was repeated at least three times and results were expressed as means ± SD.

Cell cycle analysis

Cell cycle distribution was analyzed by flow cytometry of PI staining. Briefly, HeLa cells were exposed to the tested compounds at the indicated concentrations for 24 h. Cells were collected and washed twice with PBS, then resuspended in 500 μL staining solution containing PI (10 μg mL^{-1}) and DNAse-free RNase (100 μg mL^{-1}) and analysed by flow cytometry (FACSCaliburTM, Becton Dickinson, NJ, USA). Data were analysed using ModFit LT (2.0) software (Variety Software House, Inc., Topsham, ME, USA).

Annexin V/PI assay

The assay was performed according to the manufacturer's protocol. HeLa cells cultured in 6-well plates were exposed to the tested compounds at indicated concentrations for 24 h. The cells were then collected and resuspended in 200 μL Annexin-binding buffer. The cell suspension was stained with 5 μL annexin V and 10 μL PI at room temperature for 10 min in the dark, and analyzed immediately by flow cytometry (FACSCaliburTM, Becton Dickinson, NJ, USA). Control cells stained with Annexin V-FITC or PI alone was used to compensate for the flow cytometric analysis. Resulting dot blots were quantified using FlowJo Software (Tree Star, OR, USA).

Fluorescence microscopic examination

HeLa cells were seeded in confocal dishes for 24 h and treated with the tested compounds at the indicated concentrations for 1 h, then medium was removed. Cells were washed with PBS for three times, and visualized using confocal microscopy (LSM 710, Carl Zeiss, Göttingen, Germany).

Measurement of MMP

HeLa cells were treated with the tested compounds at the indicated concentrations for 4 h. The cells were then collected and resuspended in 1 mL staining solution containing JC-1 (5 μg mL^{-1}) and incubated for 20 min at 37 °C. Subsequently, the cells were washed twice with PBS, and were analysed immediately by flow cytometry (FACSCaliburTM, Becton Dickinson, NJ, USA). Red and green populations were gated for quantification analysis using FlowJo software (Tree Star, OR, USA). Ten thousand events were acquired for each sample.

ROS detection

After treated with the tested compounds for 4 h, HeLa cells were collected by and incubated for 20 min at 37 °C with 10 μM H_2DCF-DA (Sigma Aldrich, Missouri, USA) in serum-free DMEM. The cells were washed twice with serum-free DMEM, and the fluorescence intensity of cells was measured by flow cytometry (FACSCaliburTM, Becton Dickinson, NJ, USA), with excitation set at 488 nm and emission at 530 nm. Data were analysed using FlowJo flow-cytometry software (Tree Star, OR, USA). Ten thousands events were acquired for each sample.

Caspase activity assay

Caspase activity was measured in HeLa cell lines by caspase-gloTM 3/7 assay kit (Promega). HeLa cells in 96-well culture microplates were treated with the tested compounds at an indicated time and concentration. The old medium was removed and 100 μL cell lysis (Promega) was added for 5 minutes. Then, 15 μL of sample was added to a 384-well format and subsequently incubated with 15 μL of caspase-glo 3/7 reagent (30 min). Luminescence was recorded by using a microplate reader (Infinite M200 PRO, Tecan, Switzerland). Cisplatin was used as a positive control.

Western blot

HeLa cells were seeded in 6 cm tissue-culture dishes and incubated with culture medium at 37 °C in a humidified atmosphere of 5% CO_2/95% air for 24 h, and then exposed to complexes at the indicated concentrations for 12 h. Cells were harvested and washed with ice-cold PBS twice, then were lysed in radio-immunoprecipitation assay (RIPA) buffer (200 μL, 1% Trition X-100, 10% deoxycholate, 50 mM Tris-HCl, pH 7.5, 150 mM NaCl, 0.1% SDS, 0.1 mM PMSF, 10 μg mL^{-1} leupeptin, 10 μg mL^{-1} aprotinin at 0 °C). Equal amounts of cellular total proteins (20–60 μg) were separated using SDS-polyacrylamide gel electrophoresis and then transferred onto polyvinylidene difluoride membranes (Millipore, MA, USA). Membranes were blocked in 20 mM Tris, pH 8.0, 150 mM NaCl, and 0.05% Tween 20 (TBST, Sigma Aldrich, Missouri, USA) containing 5% nonfat dried milk, and then incubated with the primary antibodies (Cell Signaling Technology, MA, USA) at 4 °C overnight. After a subsequent washing step, the membrane is incubated with the appropriate horseradish peroxidase-conjugated secondary antibody for 2 h. Detection was performed by using the chemiluminescence procedure (ECL, Amersham).

Acknowledgements

This work is supported by National Natural Science Foundation of China (21172274, 21201183, 21231007 and 21272285), the Key Project of Chinese Ministry of Education (313058), the Program for Changjiang Scholars and Innovative Research Team in University of China (IRT1298), and the State High-Tech Development Program (863 Program: 2012AA020305).

References

1 F. Cisnetti and A. Gautier, *Angew. Chem., Int. Ed.*, 2013, **52**, 11976–11978.
2 W. Henderson, B. K. Nicholson and E. R. T. Tienkink, *Inorg. Chim. Acta*, 2006, **359**, 204–214.
3 A. G. Quiroga and C. N. Ranninger, *Coord. Chem. Rev.*, 2004, **248**, 119–133.
4 W. A. Herrmann, *Angew. Chem., Int. Ed.*, 2002, **41**, 1290–1309.
5 D. Bourissou, O. Guerret, F. P. Gabbaï and G. Bertrand, *Chem. Rev.*, 2000, **100**, 39–91.
6 V. Dragutan, I. Dragutan, L. Delaude and A. Demonceau, *Coord. Chem. Rev.*, 2007, **251**, 765–794.
7 N. Marion and S. P. Nolan, *Acc. Chem. Res.*, 2008, **41**, 1440–1449.
8 H. Hu, I. Castro-Rodriguez, K. Olsen and K. Meyer, *Organometallics*, 2004, **23**, 755–764.
9 D. Nemcsok, K. Wichmann and G. Frenking, *Organometallics*, 2004, **23**, 3640–3646.
10 J. C. Garrison, R. S. Simons, J. M. Talley, C. Wesdemiotis, C. A. Tessier and W. J. Youngs, *Organometallics*, 2001, **20**, 1276–1278.
11 K. M. Hindi, M. J. Panzner, C. A. Tessier, C. L. Cannon and W. J. Youngs, *Chem. Rev.*, 2009, **109**, 3859–3884.
12 M. L. Teyssot, A. S. Jarrousse, M. Manin, A. Chevry, S. Roche, F. Norre, C. Beaudoin, L. Morel, D. Boyer, R. Mahiou and A. Gautier, *Dalton Trans.*, 2009, 6894–6902.
13 A. Gautier and F. Cisnetti, *Metallomics*, 2012, **4**, 23–32.
14 C. A. Moyer, L. Brentano, D. L. Gravens, H. W. Margraf and W. W. Monafo, *Arch. Surg.*, 1965, **90**, 812–867.
15 H. J. Klasen, *Burns*, 2000, **26**, 117–130.
16 A. Melaiye, R. S. Simons, A. Milsted, F. Pingitore, C. Wesdemiotis, C. A. Tessier and W. J. Youngs, *J. Med. Chem.*, 2004, **47**, 973–977.
17 A. Melaiye, Z. Sun, K. Hindi, A. Milsted, D. Ely, D. H. Reneker, C. A. Tessier and W. J. Youngs, *J. Am. Chem. Soc.*, 2005, **127**, 2285–2291.
18 A. Kascatan-Nebioglu, K. Melaiye, S. Hindi, M. J. Durmus, L. A. Panzner, R. J. Mallett, C. E. Hovis, M. Coughenour, S. D. Crosby, A. Milsted, D. L. Ely, C. A. Tessier, C. L. Cannon and W. J. Youngs, *J. Med. Chem.*, 2006, **49**, 6811–6818.
19 K. M. Hindi, T. J. Siciliano, S. Durmus, M. J. Panzner, D. A. Medvetz, D. V. Reddy, L. A. Hogue, C. E. Hovis, J. K. Hilliard, R. J. Mallet, C. A. Tessier, C. L. Cannon and W. J. Youngs, *J. Med. Chem.*, 2008, **51**, 1577–1583.
20 W. J. Youngs, A. R. Knapp, P. O. Wagers and C. A. Tessier, *Dalton Trans.*, 2012, **41**, 327–336.

21 S. Roland, C. Jolivat, T. Cresteil, L. Eloy, P. Bouhours, A. Hequet, V. Mansuy, C. Vanucci and J.-M. Paris, *Chem. – Eur. J.*, 2011, **17**, 1442–1446.
22 B. Thati, A. Noble, B. S. Creaven, M. Walsh, M. McCann, K. Kavanagh, M. Devereux and D. A. Egan, *Cancer Lett.*, 2007, **248**, 321–331.
23 H. L. Zhu, X. M. Zhang, X. Y. Liu, X. J. Wang, G. F. Liu, A. Usman and H. K. Fun, *Inorg. Chem. Commun.*, 2003, **6**, 1113–1116.
24 J. J. Liu, P. Galettis, A. Farr, L. Mahraj, H. Samarasinha, A. C. McGechan, B. C. Baguley, R. J. Bowen, S. J. Berners-Price and M. J. McKeage, *J. Inorg. Biochem.*, 2008, **102**, 303–310.
25 S. E. H. Etaiw, A. S. Sultan and A. S. Badr El-din, *Eur. J. Med. Chem.*, 2011, **46**, 5370–5378.
26 D. A. Medvetz, K. M. Hindi, M. J. Panzner, A. J. Ditto, Y. H. Yun and W. J. Youngs, *Met.-Based Drugs*, 2008, 384010.
27 D. C. F. Monteiro, R. M. Phillips, B. D. Crossley, J. Fieldena and C. E. Willans, *Dalton Trans.*, 2012, **41**, 3720–3725.
28 W. Liu and R. Gust, *Chem. Soc. Rev.*, 2013, **42**, 755–773.
29 S. S. Gunatilleke and A. M. Barrios, *J. Med. Chem.*, 2006, **49**, 3933–3937.
30 J. Talib, J. L. Beck and S. F. Ralph, *JBIC, J. Biol. Inorg. Chem.*, 2006, **11**, 559–570.
31 İ. Özdemir, A. Denizci, H. T. Öztürk and B. Çetinkaya, *Appl. Organomet. Chem.*, 2004, **18**, 318–322.
32 M. M. Jellicoe, S. J. Nichols, B. A. Callus, M. V. Baker, P. J. Barnard, S. J. Berners-Price, J. Whelan, G. C. Yeoh and A. Filipovska, *Carcinogenesis*, 2008, **29**, 1124–1133.
33 J. J. Yan, A. L.-F. Chow, C.-H. Leung, R. W.-Y. Sun, D.-L. Ma and C.-M. Che, *Chem. Commun.*, 2010, **46**, 3893–3895.
34 C.-H. Wang, W.-C. Shih, H. C. Chang, Y.-Y. Kuo, W.-C. Hung, T.-G. Ong and W.-S. Li, *J. Med. Chem.*, 2011, **54**, 5245–5249.
35 W. Liu, K. Bensdorf, M. Proetto, U. Abram, A. Hagenbach and R. Gust, *J. Med. Chem.*, 2011, **54**, 8605–8615.
36 R. Rubbiani, S. Can, I. Kitanovic, H. Alborzinia, M. Stefanopoulou, M. Kokoschka, S. Mönchgesang, W. S. Sheldrick, S. Wölfl and I. Ott, *J. Med. Chem.*, 2011, **54**, 8646–8657.
37 R. Rubbiani, I. Kitanovic, H. Alborzinia, S. Can, A. Kitanovic, L. A. Onambele, M. Stefanopoulou, Y. Geldmacher, W. S. Sheldrick, G. Wolber, A. Prokop, S. Wölfl and I. Ott, *J. Med. Chem.*, 2010, **53**, 8608–8618.
38 W. K. Liu, K. Bensdorf, M. Proetto, A. Hagenbach, U. Abram and R. Gust, *J. Med. Chem.*, 2012, **55**, 3713–3724.
39 E. Schuh, C. Pflüger, A. Citta, A. Folda, M. P. Rigobello, A. Bindoli, A. Casini and F. Mohr, *J. Med. Chem.*, 2012, **55**, 5518–5528.
40 T. Zou, C. T. Lum, S. S.-Y. Chui and C.-M. Che, *Angew. Chem., Int. Ed.*, 2013, **52**, 2930–2933.
41 P. J. Barnard and S. J. Berners-Price, *Coord. Chem. Rev.*, 2007, **251**, 1889–1902.
42 S. J. Berners-Price and A. Filipovska, *Aust. J. Chem.*, 2008, **61**, 661–668.
43 S. J. Berners-Price and A. Filipovska, *Metallomics*, 2011, **3**, 863–873.
44 M. V. Baker, B. W. Skelton, A. H. White and C. C. Williams, *J. Chem. Soc., Dalton Trans.*, 2001, 111–120.
45 H. M. J. Wang and I. J. B. Lin, *Organometallics*, 1998, **17**, 972–975.
46 M. Pellei, V. Gandin, M. Marinelli, C. Marzano, M. Yousufuddin, H. V. R. Dias and C. Santini, *Inorg. Chem.*, 2012, **51**, 9873–9882.
47 O. Hollóczki, P. Terleczky, D. Szieberth, G. Mourgas, D. Gudat and L. Nyulászi, *J. Am. Chem. Soc.*, 2011, **133**, 780–789.
48 P. J. Barnard, M. V. Baker, S. J. Berners-Price and D. A. Day, *J. Inorg. Biochem.*, 2004, **98**, 1642–1647.
49 L. Eloy, A.-S. Jarrousse, M.-L. Teyssot, A. Gautier, L. Morel, C. Jolivalt, T. Cresteil and S. Roland, *ChemMedChem*, 2012, **7**, 805–814.
50 J. L. Hickey, R. A. Ruhayel, P. J. Barnard, M. V. Baker, S. J. Berners-Price and A. Filipovska, *J. Am. Chem. Soc.*, 2008, **130**, 12570–12571.
51 R. W.-Y. Sun, A. L.-F. Chow, X.-H. Li, J. J. Yan, S. S.-Y. Chui and C.-M. Che, *Chem. Sci.*, 2011, **2**, 728–736.
52 P. J. Barnard, L. E. Wedlock, M. V. Baker, S. J. Berners-Price, D. A. Joyce, B. W. Skelton and J. H. Steer, *Angew. Chem., Int. Ed.*, 2006, **45**, 5966–5970.
53 T. Zou, C.-N. Lok, Y. M. E. Fung and C.-M. Che, *Chem. Commun.*, 2013, **49**, 5423–5425.
54 R. Rubbiani, E. Schuh, A. Meyer, J. Lemke, J. Wimberg, N. Metzler-Nolte, F. Meyer, F. Mohr and I. Ott, *MedChemComm*, 2013, **4**, 942–948.
55 S. Ray, R. Mohan, J. K. Singh, M. K. Samantaray, M. M. Shaikh, D. Panda and P. Ghosh, *J. Am. Chem. Soc.*, 2007, **129**, 15042–15053.
56 M.-L. Teyssot, A. S. Jarrousse, A. Chevry, A. De Haze, C. Beaudoin, M. Manin, S. P. Nolan, S. Díez-González, L. Morel and A. Gautier, *Chem. – Eur. J.*, 2009, **15**, 314–318.
57 R. C. Taylor, S. P. Cullen and S. J. Martin, *Nat. Rev. Mol. Cell Biol.*, 2008, **9**, 231–241.
58 S. D. Adhikary, D. Bose, P. Mitra, K. D. Saha, V. Bertolasi and J. Dinda, *New J. Chem.*, 2012, **36**, 759–767.
59 H. Sivaram, J. Tan and H. V. Huynh, *Organometallics*, 2012, **31**, 5875–5883.
60 I. Vermes, C. Haanen and C. Reutelingsperger, *J. Immunol. Methods*, 2000, **243**, 167–190.
61 C.-M. Che and R. W.-Y. Sun, *Chem. Commun.*, 2011, **47**, 9554–9560.
62 M. V. Stankov, T. Lücke, A. M. Das, R. E. Schmidt and G. M. Behrens, *Antimicrob. Agents Chemother.*, 2010, **54**, 280–287.
63 D. Trachootham, J. Alexandre and P. Huang, *Nat. Rev. Drug Discovery*, 2009, **8**, 579–591.
64 R. U. Janicke, M. L. Sprengart, M. R. Wati and A. G. Porter, *J. Biol. Chem.*, 1998, **273**, 9357–9360.
65 M. V. Baker, M. J. Bosnich, D. H. Brown, L. T. Byrne, V. J. Hesler, B. W. Skelton, A. H. White and C. C. Williams, *J. Org. Chem.*, 2004, **69**, 7640–7652.
66 B. Altava, M. I. Burguete, B. Escuder, S. V. Luis, E. García-España and M. C. Muñoz, *Tetrahedron*, 1997, **53**, 2629–2640.
67 M. Zhang, A. Abdukader, Y. Fu and C. Zhu, *Molecules*, 2012, **17**, 2812–2822.

